

Article

River Flow Measurements Utilizing UAV-Based Surface Velocimetry and Bathymetry Coupled with Sonar

Paschalis Koutalakis * and George N. Zaimis

Geomorphology, Edaphology and Riparian Areas Lab (GERi Lab), Department of Forestry and Natural Environment Science, International Hellenic University, University Campus, 1st km Dramas-Mikrohorion, 66100 Drama, Greece

* Correspondence: koutalakis_p@yahoo.gr

Abstract: Water velocity and discharge are essential parameters for monitoring water resources sustainably. Datasets acquired from Unoccupied Aerial Systems (UAS) allow for river monitoring at high spatial and temporal resolution, and may be the only alternative in areas that are difficult to access. Image or video-based methods for river flow monitoring have become very popular since they are not time-consuming or expensive in contrast to traditional methods. This study presents a non-contact methodology to estimate streamflow based on data collected from UAS. Both surface velocity and river geometry are measured directly in field conditions via the UAS while streamflow is estimated with a new technique. Specifically, surface velocity is estimated by using image-based velocimetry software while river bathymetry is measured with a floating sonar, tethered like a pendulum to the UAV. Traditional field measurements were collected along the same cross-section of the Aggitis River in Greece in order to assess the accuracy of the remotely sensed velocities, depths, and discharges. Overall, the new technique is very promising for providing accurate UAV-based streamflow results compared to the field data.

Keywords: hydrologic monitoring; image-based velocimetry; river; sonar; surface velocity; streamflow; unmanned aerial vehicle; water depth; water discharge; water level



Citation: Koutalakis, P.; Zaimis, G.N. River Flow Measurements Utilizing UAV-Based Surface Velocimetry and Bathymetry Coupled with Sonar. *Hydrology* **2022**, *9*, 148. <https://doi.org/10.3390/hydrology9080148>

Academic Editor: Aronne Armanini

Received: 31 July 2022

Accepted: 14 August 2022

Published: 17 August 2022

Publisher's Note: MDPI stays neutral with regard to jurisdictional claims in published maps and institutional affiliations.



Copyright: © 2022 by the authors. Licensee MDPI, Basel, Switzerland. This article is an open access article distributed under the terms and conditions of the Creative Commons Attribution (CC BY) license (<https://creativecommons.org/licenses/by/4.0/>).

1. Introduction

Water velocity and streamflow (or water discharge) are fundamental parameters utilized to describe the hydrologic regime characteristics; thus, are necessary parameters for sustainable water resources management plans, flood warning systems, conservation and protection structures, implementation of nature-based solutions, etc., [1–3]. Various hydraulic structures are used to estimate the streamflow by measuring the water level e.g., depth water scale or stilling wells [4], flumes either Venturi or Parshall [5], and bubblers based on the pressure (in psi) [6]. A common field method is the velocity meter. The river cross-section is typically divided into subsections (see Figure 1). In each subsection, the water depth and average flow velocity are measured to obtain the water discharge [7,8]. Another commonly used traditional flow monitoring method is the establishment of a rating curve between the water level and the streamflow in order to indirectly estimate the discharge by real-time water level measurement measures [9]. It is important to note, that the river's cross sections (depth and width, area) may change over time due to vegetation growth and river-bed erosion and deposition and this implies the need for additional time and effort for the frequent monitoring to be accurate [10]. This is why in many cases streamflow measurements are taken at a stable cross-section (e.g., under a bridge or culvert). These approaches demand specialized personnel and also are time-consuming. In addition, the flow measurements in flood events are difficult (typically impossible) as there is considerable risk for the operator in high water discharges [11,12]. In such extreme events, they are not enough data points for the rating curve approach; so consequently, the curve cannot be extrapolated [13]. Other typical methods,

including Acoustic Doppler Current Profiler (ADCP) [14,15], Acoustic Doppler Velocimeter (ADV) [16,17], high-frequency Doppler radars [18,19], and remote sensing observations via satellite or airborne images [20,21], have been widely applied. These methods also require expensive equipment, laboratory work, and highly expert personnel. Furthermore, hydrologic and hydraulic modeling is another method that can provide hydrographs but requires long-term observed field datasets for their proper calibration and validation of the models [22,23].

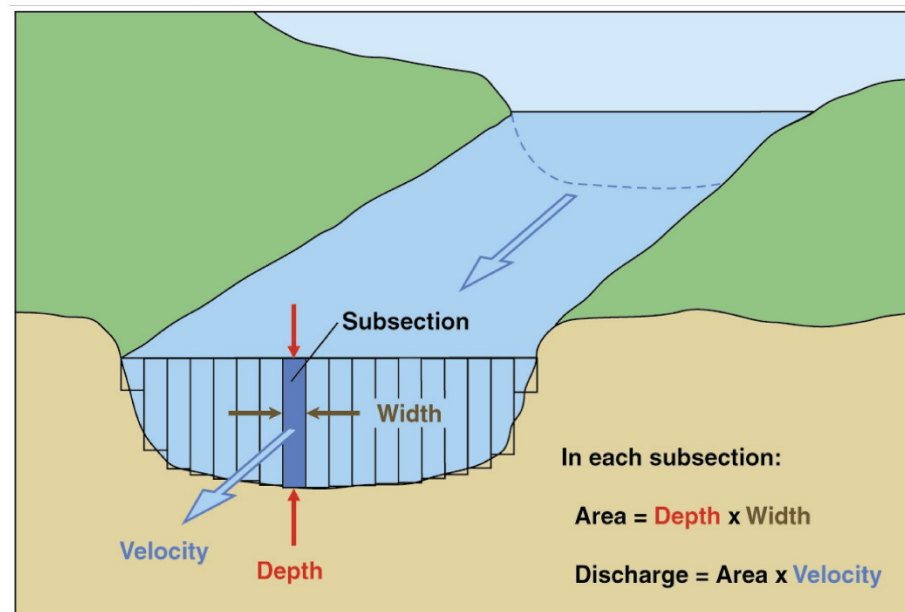


Figure 1. Diagram of channel cross section with subsections. The most common method used by the USGS for measuring velocity is with a current meter. However, a variety of advanced equipment can also be used to sense stage and measure streamflow. In the simplest method, a current meter turns with the flow of the river or stream. The current meter is used to measure water velocity at predetermined points (subsection) along a marked line, suspended cableway, or bridge across a river or stream. The depth of the water is also measured at each point. These velocity and depth measurements are used to compute the total volume of water flowing past the line during a specific interval of time. Usually, a river or stream will be measured at 25 to 30 regularly spaced locations across the river or stream. Source: USGS Public Domain.

Nowadays, image-based techniques have proved to be a popular and reliable non-intrusive method to measure hydrological parameters for river monitoring [24]. These methods allow easy, low-cost, and real-time measurements at any flow conditions and at high spatial resolution [25]. Image-based velocimetry is an optical method that computes surface water velocity maps from videos (or extracted time frames) recorded by a camera [26]. Surface tracers are detected and tracked in order to measure the distances and time; thus, directly calculating the surface velocity vectors [27]. Applications with different image-based velocimetry (IV) methodologies (different approaches/formulas) have been exploited by researchers worldwide. Among the various image-based methods [28–31], there are two different approaches that have been widely accepted in monitoring the velocity of natural rivers: (a) the large-scale particle image velocimetry (LSPIV) and (b) the large-scale particle tracking velocimetry (LSPTV). Both techniques were originally developed for laboratory experiments under controlled conditions as particle image velocimetry (PIV) and particle tracking velocimetry (PTV) techniques [32]. Their further implementation in natural conditions has led to the addition of the term “large-scale”.

These image-based techniques use the frames captured by a video, in order to analyze the movement of floating tracers on the water surface and in this way estimate the surface velocity of the fluid. LSPIV adopts the Eulerian approach and estimates the velocity at

image sub-regions, while LSPTV uses the Lagrangian approach to reconstruct the trajectory of individual particles transiting in the field of view [33]. Both techniques (LSPIV and LSPTV) have rapidly evolved due to the new generation of optical sensors, digital cameras, and methodologies as well as the decrease in their cost that has made them affordable to a wider audience [34,35]. Finally, specialized cameras (e.g., thermal imaging or night vision) have been used to eliminate the disadvantage of image recording during the night [36,37].

The establishment of ground control points (GCPs), or ground reference points (GRPs), as benchmarks is a necessary step in oblique imagery [38]. This step is required in order to ortho-rectify the images when the camera is positioned at an oblique angle in contrast to the water surface [39]. This technique induces the error of the perspective distortion which is the direct result of the camera placement in relation to an object. Objects which are closer to the camera always appear larger than those further away. In these cases, image correction and ortho-rectification are required, especially when the imaging device cannot be oriented rectangularly on the water surface or when the camera lens produces extremely distorted images, as is the case with fish-eye lenses [40]. Generally, at least 4 GCPs are acquired for image calibration and ortho-rectification, thus the area must be accessible to human operators [41]. The images are ortho-rectified using the GCPs and are assigned in real metric dimensions. Proper image correction, often recorded at an oblique angle, is one of the biggest challenges, but recently very promising results have been achieved [42]. Tauro et al. (2014) performed experiments by using laser pointers on permanent gauges to estimate true distances in the image domain and to avoid the usage of GCPs [43]. Le Coz et al. (2010) used a mobile LSPIV system which consisted of a digital video camera (Canon MV750i) set on a mobile telescopic mast whose height could be set from 2 to 10 m [44]. The camera was remotely controlled from the ground, in order to adjust view angles. For each test, 10 GCPs (white and red 40 cm by 40 cm square targets) were positioned along both banks of the river.

Recently, the implementation of image-based monitoring by utilizing unoccupied (or unmanned) aerial systems (UASs) has increased [45–48]. The acronym “IV-UAV” was proposed to describe the image-based methodology and distinguish it from those applied through other means (not UAVs) [49]. IV-UAV has been proved as an efficient and powerful technique for measuring river surface velocities worldwide [50–52]. There are many advantages they offer in contrast to other relevant techniques for natural river monitoring. For instance, image-based methods work well in the case of shallow flows to reconstruct rating curves and estimate discharge in riverine systems, enabling flow field measurements rather than point-wise estimations, the instrumentation is of low-cost in contrast to other practices and the streamflow monitoring/recording is a fully remote procedure to avoid dangerous conditions through water contact [53–55]. Additionally, in some cases (e.g., inaccessible areas), the IV-UAV method may be the only realistically available for streamflow measurements. The UAVs, which contain a GPS/GNSS system, greatly increased the flexibility of the camera location and imaging height. Tauro et al. (2016) experimented with a system of lasers equipped on a tetra copter UAV which enabled remote photometric calibration without the need for time-consuming and expensive field campaigns for GRPs acquisition [56]. If tilt and lens distortion effects on resultant velocities are small, time-consuming control-point surveys may not be required [57]. This is achievable, since the cameras which are mounted on UAV platforms can be maintained in a vertical position due to their GPS/GNSS system, intensive rectification of imagery due to image distortion and tilt is not always required [58]. A perpendicular or nearly perpendicular orientation of the optical axes of these instruments in relation to the water surface (when the plane of view of the UAV’s camera is parallel and flat to the XY plane), means that the ortho-rectification of images is not required as the drone x, y position is equal to the x, y position of the center of the image. [59–61]. The motorized gimbal on the UAS ensures that the camera is nearly orthogonal to the ground surface once the gimbal has been calibrated in reference to a flat surface. The concern arises when wind velocity is increased, and the hovering position cannot be stable (or even difficult to fly) and the

application should be avoided. During rapid UAS movement or high winds, the camera may briefly tilt to a minor degree, but within fractions of a second, the gimbal returns the camera to an orthogonal perspective [62]. Additionally, this error is minimized when flying on a “tripod” mode which promotes stable and slow UAV hovering. An alternative way is to extract the video frames which do not present any distortion (part of the video which is stable). In other cases, if the distortion is visible and must be removed, there are many free or commercial software that can be used to minimize the induced errors because of the lens distortion [63]. In general, lens distortion can be grouped into automatic or library-based and manual-based distortion removal. As the name entails, the automatic distortion removal does not require great input from the user and is relied on the distortion removal on a library of known lens profiles [64]. Finally, the method employs parameters and settings that require an expert background in image/video analysis (e.g., interrogation area size, and cross-correlation parameters). These parameters are related to the specific field conditions (e.g., height of flight, seeding density, tracers’ dimension, frame rate) and may not be easily identifiable [65].

Limited research has been conducted to combine the IV-UAV method with a floating sonar for water level/depth measurements in order to estimate the streamflow. This study is an attempt to fill in this scientific gap. Sonar (Sound Navigation and Ranging), LiDAR (Light Detection and Ranging), multimedia stereo-photogrammetry, and spectrally derived bathymetry (SDB) have proved very suitable for bathymetric mapping [66]. Sonars can reach large depth penetration while optical remote sensing methods are most suitable for shallow waters [67]. Recently, Lin et al. (2022) applied the LSPIV method on shallow waters (circulated flume) while the two-dimensional bathymetry in laboratory conditions was estimated from the depth-averaged velocity and the continuity equation with the leapfrog scheme in a predefined grid under the constraints of Courant–Friedrichs–Lewy (CFL) [68]. Various UAV-based systems (with sonars or not) have been developed for nearshore or marine bathymetry monitoring [69,70]. Sanjou et al. (2022) utilized recently a drone-type float with a Global Positioning System (GPS) receiver in order to detect the time-series of self-position with a centimeter-order accuracy. In addition, an attached ultrasonic sensor enabled the measurement of the local water depth [71]. By integrating data acquired by unmanned surface vehicles (USVs) and UAVs a uniform bathymetric surface of a shoreline was created [72]. A combination of sensors on an aerial drone, floating drone, and underwater drone were utilized for bathymetric monitoring of reservoirs [73]. UAVs in combination with ADCP and GPS were applied for river bathymetry modelling based on optical remote sensing [74]. Bandini et al. [10] performed novel research by attaching a commercially available fishing sonar (Deeper Smart Sonar Pro+), via a winch mechanism, to a DJI Spreading Wings S9000 hexa-copter [75]. Finally, Ruffel et al. (2021) also used a lightweight sonar device tethered to a UAV to easily measure the water depth by applying river scanning [76]. This study follows the concept of the previous work of Bandini [77] by combining (a) the IV-UAV method for surface velocity estimation and (b) a UAV-tethered sonar for river depth estimation to eventually estimate the river discharge. This combination should increase the accuracy of discharge measurements by capturing in great detail the channel form, and estimating stream velocity, cost-effectively and non-intrusively.

2. Materials and Methods

2.1. The Study Site

Aggitis Basin is located in the prefecture of Eastern Macedonia in Northern Greece. The study site was a reach of Aggitis River (Figure 2). Aggitis (or Angitis) River is the main water course that contributes to the Strymonas River that finally discharges to the Strymonikos Gulf in the North Aegean Sea [78]. The Aggitis basin is surrounded by the Menoikio Mountain at the west, Falakro Mountain at the east, and from the Ori Lekanis and Paggeo Mountains at the southeast and southwest borders of the basin, respectively [79]. The hydrographic network is mainly characterized as a dendritic while in some areas it

can be characterized as a more complex network form [80]. These areas are located in the southern part of Mount Menoikio where due to the gorge of “Stena Petras” close to Alistrati caves, the network shows a hybrid dendritic and parallel form. The same form of the hydrographic network appears in branches of the Falakro Mountain, probably due to the large slopes ($>45^\circ$) and the lithological formations in the area. In the whole floodplain area of the Aggitis Basin, there is an extensive surface drainage/irrigation network including the drainage ditch of the Tenagi Philippon [81]. Flood events are a frequent phenomenon in the Aggitis Basin [82], especially in the area of Tenagi-Philippoi, but also in the floodplains of the local torrents which are the dominant water course type in the area. The specifically studied cross-section is located near Simvoli Village; the name “simvoli” (in Greek) means “confluence” (Figure 3) to describe the conjunction of Aggitis River with Agia Barbara stream and Xiropotamos stream (the last is the irrigation channel of Tenagi Philippon and the Doxato stream). In the confluence location, a dam with movable gates was constructed in 1930 in order to regulate the flow when extreme events occur and for irrigation purposes. The highest flow of Aggitis that was measured (at the exit from the gorge of the same name) is $100 \text{ m}^3/\text{s}$ (28-2-1931). Jackson estimated the maximum flow of Aggitis, at the point of entry into the gorge of the same name (Simvoli dam) equaled $1040 \text{ m}^3/\text{s}$, for the basin’s area of 1630 km^2 [83].

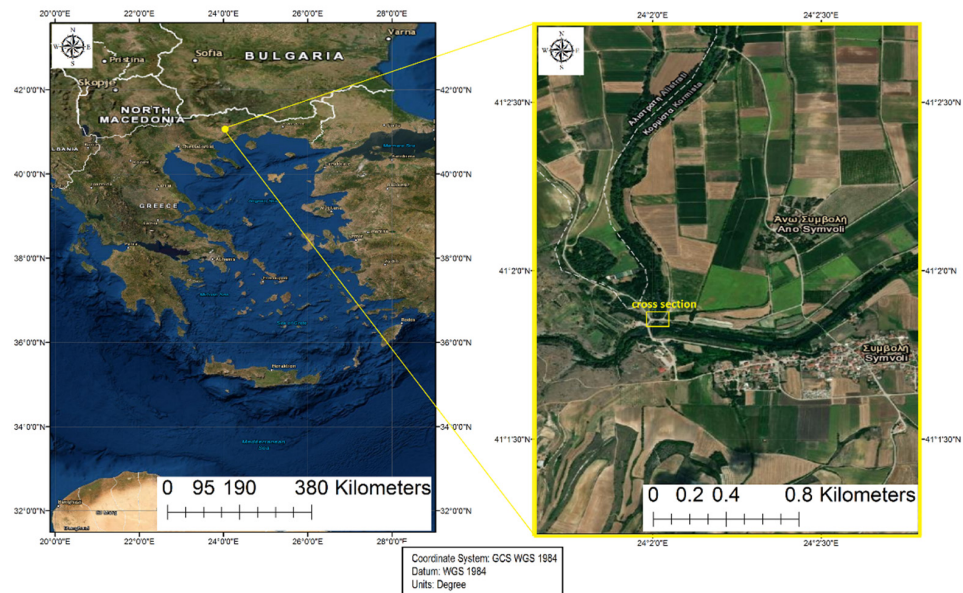


Figure 2. The studied reach is located near Simvoli Village in relation to Greece (in yellow). This is the confluence of Aggitis River with Agia Barbara stream and Xiropotamos stream.



Figure 3. A photo of the studied reach. It is the confluence of Aggitis River with Agia Barbara stream and Xiropotamos stream. The different color of the river’s water was due to the different rainfall events in the sub-watersheds. The dam with its movable gates is also depicted on the right of the picture.

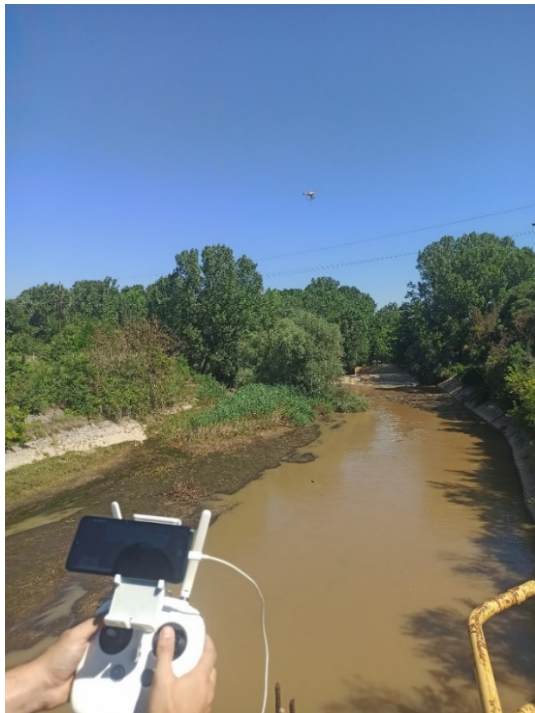
2.2. The Innovative Method

2.2.1. The Hardware

In this research, the DJI Phantom 4 Pro (Figure 4) hovered at 20 m over the selected location and captured a short video (30 s) in the “tripod flight mode” of the surface water flow. Liu et al. (2021), proved that there are slight differences during low flow conditions and at relatively low heights (e.g., 10–20 m) [84]. In their study, the flight height was adequate to capture the natural surface tracers (bubbles) and to include the riverbanks in the studied frame in order to measure the GCPs [84]. The drone hovered by using its remote controller, able to fly away (the signal range is close to 7 km) from the pilot; but for the needs of this study and for safety rules, the pilot was in close range to the UAV platform (Figure 5). The UAV camera was set to perpendicular orientation in relation to the water surface to avoid ortho-rectification. The photos’ resolution was 1920×1080 , while the shooting speed of the images was 30 frames per second (fps). The specifications of the drone are depicted in Table 1 [85]. Bathymetry measurements were performed at a second similar flight, by coupling this time a tethered sonar (the Deeper Smart Sonar PRO), specifically, by tying the spherical tool likewise with a fish hook (see Figures 4 and 5b). Bathymetry sonars always need to be positioned in contact with the water surface. The specific device is a versatile and powerful sonar scans to a depth of 80 meters, using its secure Wi-Fi connection to send detailed information directly to your smartphone or tablet [86]. It is used mainly for fishing, as it marks the fish, locates underwater structures and elements, and maps the terrains of the waterbody from a kayak/boat [87]. Recently, it was utilized in order to estimate the volume of lakes and reservoirs based on aquatic drone surveys [88]. The results obtained through the described UAV-Sonar-based methodology were further validated (a) by traditional cross-section survey (field measurements applying a tape measure and streamflow measurement via a propeller streamflow meter; see Figure 6a,b) and (b) by the measurements recorded by an installed telemetric hydrological station RSS-2-300 WL (Geolux Ltd. Zagreb, Croatia) able to measure the surface velocity and water depth at the current location. In addition, an installed water-level meter at the dam was used to validate the bathymetric measurements (Figure 7a). Finally, the GCPs for geo-rectification were measured by the GPS-GNSS antenna RTK “RUIDE NOVA R6” (GPS, GLONASS, BeiDou, Galileo, SBAS) (SOUTH Group, Ruide Surveying Instrument Co., Ltd., Guangzhou, China) (see Figure 7b).



Figure 4. The DJI Phantom 4 Pro Unmanned Aerial Vehicle (UAV) coupled with the tethered sonar (Deeper Smart Sonar PRO) for the bathymetric measurements.



(a)



(b)

Figure 5. (a) The remote controller of the DJI Phantom 4 Pro attached to the smartphone with the DJI GO 4 app; (b) the UAV flight and the sonar in contact with the water surface.

Table 1. The specifications of DJI Phantom 4 Pro based on its official website (<https://www.dji.com>, accessed on 15 July 2022).

| Drone Specifications (Aircraft and Camera) for the DJI Phantom 4 Pro | |
|---|---|
| Weight: | 1388 g |
| Diagonal size (no propellers): | 350 mm |
| Max flight time: | 30' |
| Max speed (sport/A mode/P mode): | 72 km/h/58 km/h/50 km/h |
| Satellite positioning: | GPS/GLONASS (both) |
| Hover accuracy range: | Vertical ± 0.1 m and Horizontal ± 0.3 m |
| Battery capacity: | 5870 mAh LiPo 4S 15.2V |
| Supported SD Cards | Micro SD \leq 128GB |
| Camera Sensor: | 1" CMOS |
| Effective pixels: | 20 million |
| Lens (FOV): | FOV 84° 8.8 mm/24 mm (35 mm format equivalent) |
| ISO range Photo: | 100–3200 (Auto) & 100–12,800 (Manual) |
| Still Photography Modes | Single Shot, Burst Shooting, Interval, Auto Exposure Bracketing |
| Photo Format: | JPEG, DNG (RAW), JPEG + DNG |
| Video Format: | MP4/MOV (AVC/H.264; HEVC/H.265) |
| Image size: | (4:3) 4864 \times 3648 & (16:9) 5472 \times 3078 |
| Gimbal Stabilization: | 3-axis (pitch, roll, yaw) |
| Shutter Speed | 8–1/2000s (mechanical) & 8–1/8000s (electronically) |
| Remote controller Operating Frequency: | 2.400–2.483 GHz and 5.725–5.825 GHz |
| Operating Temperature Range | 32° to 104°F (0° to 40°C) |
| Remote controller Battery | 6000 mAh LiPo 2S |
| Mobile Device Holder | 5.5', 1920 \times 1080, Android system (Tablets and smart phones), 4 GB RAM + 16 GB ROM |

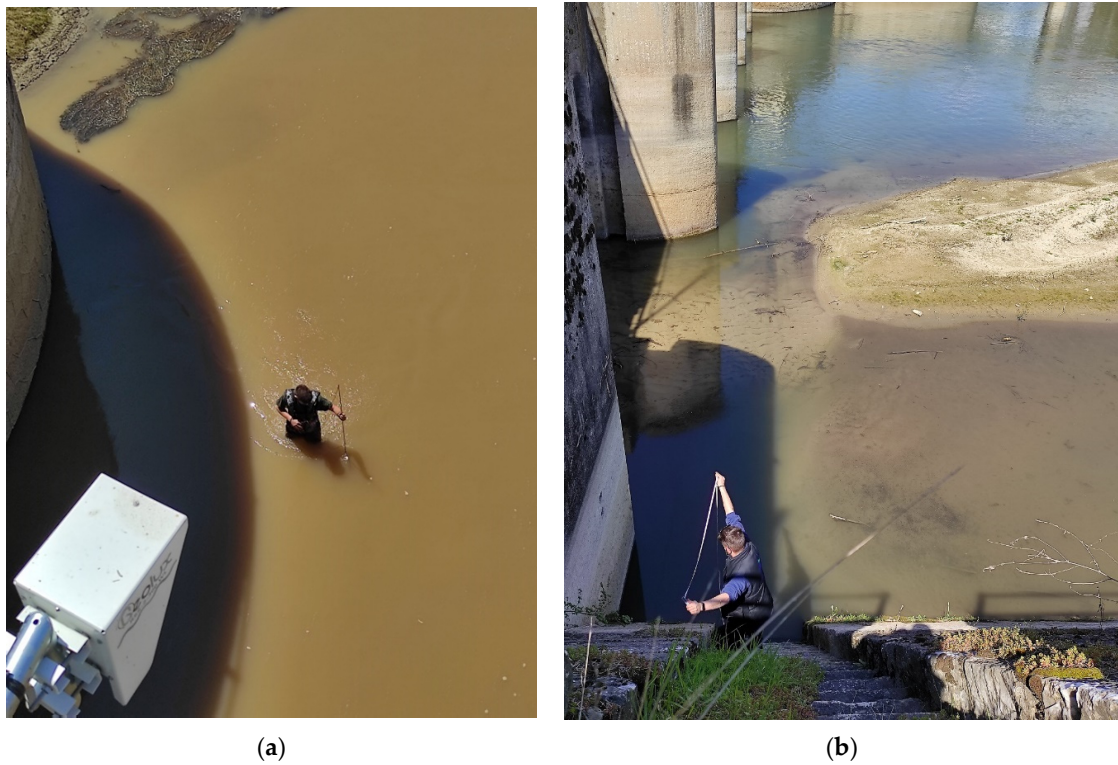


Figure 6. (a) The streamflow measurements utilizing a streamflow meter; (b) using a tape measure for the water depth validation.



Figure 7. (a) an installed water level meter at the gates of the dam that recorded a water depth 0.7 m; (b) the GPS-GNSS antenna RTK "RUIDE NOVA R6" used to obtain the coordinates of the area.

2.2.2. The Software

The software used in this study is recorded in Table 2. The UAV was controlled from its official smartphone application DJI GO 4. The images from the UAV and the terrestrial fixed station were stabilized for the IV-UAV analysis. A good example of automatic distortion removal is the commercial software PTLens; one of the most-used tools because it provides a graphical Windows interface, a vast camera/lens database, good accuracy, and a reasonable price [89]. Hugin is a panorama stitcher, graphical user interface (GUI) for Panorama tools, and like other GUI front-ends, included a range of advanced features e.g., lens distortion correction [90]. In this study firstly, the captured video was pre-processed for the reduction of various undesired errors such as lens distortion and shaking of the camera (shift, rotation, and focus). PTLens and Hugin software were utilized to remove lens distortion while tilt (if appeared) was removed by using the “Deshaker Toolbox.” The Deshaker toolbox was written by Gunnar Thalin as a widely recognized image stabilizer plugin produced for the popular video player VirtualDub [91]. This toolbox generates an output file of the estimated rigid body translations and rotations for all frames [92]. In addition, this tool uses a high-performance image-based approach for stabilization, where movement is estimated iteratively using a multi-resolution search (matching algorithm), so that large movements can be calculated to high precision using the fewest possible calculations [93]. Deshaker processes the video in two phases: (a) determines optimum parameters and (b) stabilizes the video. The KMPlayer software is capable to extract the frames from the video. The consecutive frames of the video were exported in images of 8bits (black and white color) via the KMPlayer software developed by Pandora TV; a well-known multimedia player that can play movies, music, and more. The images are greyscale for better and quicker estimations. To perform the analysis, a part of all frames was selected that covered a period of a few seconds from the video, based on the minimum displacement among the control points. The time step was set at 33.33 ms based on the video’s frame rate of 30 fps.

Table 2. The software used in the proposed coupled method.

| Software | Purpose | Developer |
|-----------------|---|---|
| DJI GO 4 App | UAV flight & record video | Da-Jiang Innovations (DJI) |
| PTLens | Lens distortion of video | Tom Niemann-ePaperPress |
| Hugin | Lens distortion of video | SourceForge |
| Deshaker | Tilt correction of video | Gunnar Thalin |
| PIVlab | Image analysis for the surface velocity results | William Thielicke and Eize J. Stamhuis |
| RIVeR | Rectification of images | Antoine Patalano Center for Water Research and Technology, National University of Cordoba, Argentina. |
| Fish Deeper App | Record and visualize bathymetric results | Deeper |

Many user-friendly software programs are widely and freely available for image-based velocimetry analysis, e.g., FlowManager, FUDAA-LSPIV, PIVlab, PTVlab, etc. [94]. The selected software for the image-based analysis was PIVlab [95], an open-source and user-friendly tool of MATLAB, which has gained considerable attention for natural river flow monitoring by many researchers [96,97]. Further pre-image editing was achieved through the PIVlab which was used for the analysis of the captured frames. Rectification of Image Velocimetry Results (RIVeR) is a complementary software to PIVlab and PTVlab; suitable for fast processing on the rectification of the velocity vectors, especially when video stabilization is not needed e.g., with fixed monitoring cameras [98]. The removal of the video frame distortion requires a long time to be performed. For vector rectification, a minimum number of GCPs are required to be measured in the field during the survey

and next aligned on the video frame during the processing phase; thus, could increase the overall time. Furthermore, RIVeR does not implement any tools for the accuracy assessment of the rectification [99]. The interrogation area window size in PIVLab was set to two passes to decrease gradually the pixels for the image-based analysis algorithm: (a) from 64 to 32 and (b) from 32 to 16. The PIV algorithm used was the Fast-Fourier's Transformation, in linear window deformation, and the sub-pixel estimator was set to Gauss 2×3 point. The image pre-processing included by default the contrast-limited adaptive histogram equalization (CLAHE) which locally enhances the contrast in the images with a window size of 20 pixels for the image analysis. Finally, the recording and visualization of the bathymetric measurements were done using the Fish Deeper application using a tablet device. The overall steps of the methodology are presented in Figure 8.

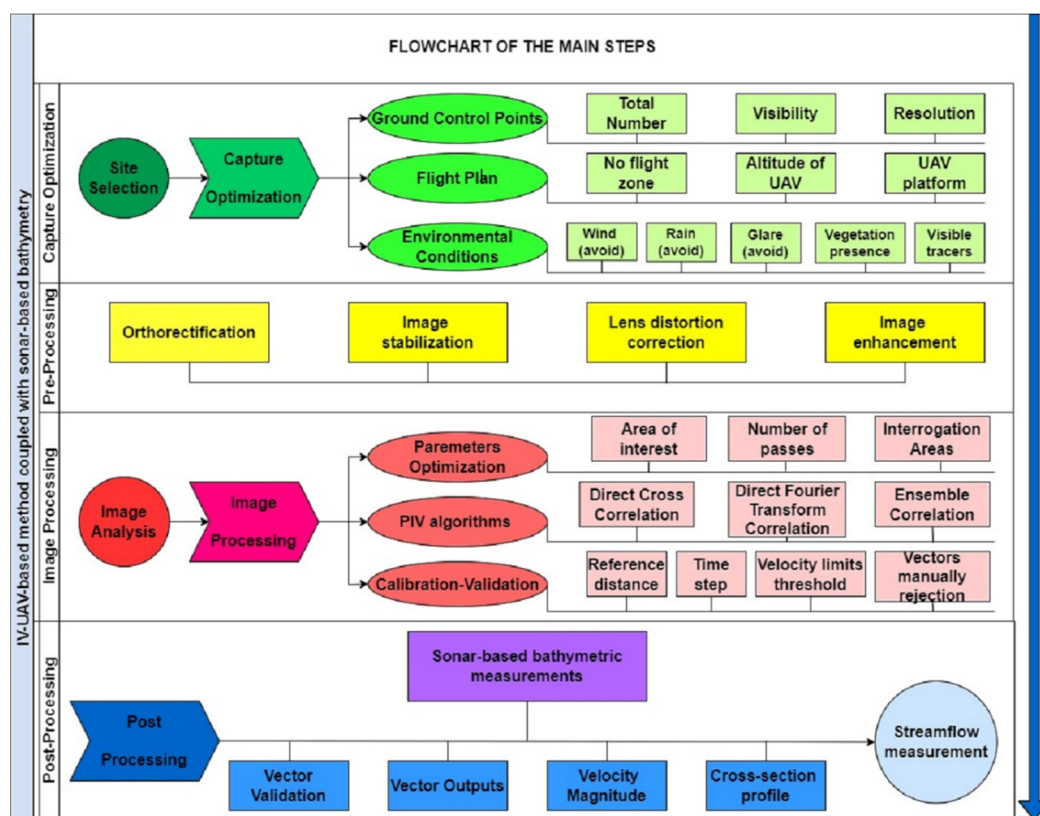


Figure 8. The flowchart of the methodology including the main preparation, pre-processing, analysis and post-processing steps.

3. Results

The studied reach that was captured parallel to XY plane by the UAV can be seen in Figure 9. The red line represents a cross-section of the bridge that is used for the calibration of the image. The real distance of this cross-section is 18 m. The results from the analysis in PIVlab depicting in green color the vectors of the surface velocity are visualized in Figure 10. The direction of the flow (as depicted in the image) is from the bottom towards the upper part of the photo as it flows under the bridge to reach the gates of the dam. The red line represents a cross-section of Aggitis River in order to visualize the surface velocity range from the left bank to the right one (see Figure 11). The faster flow path is at the right passage of the bridge where surface velocity exceeds the value of 1 m/s while there are two places (bridge pillars) where the velocity is zero (as expected). The range of the mean surface velocity is depicted in a colorized scale from 0 (dark blue) to 1.5 m/s (dark red); (see Figure 12). The mean surface velocity at the selected cross-section was 0.85 m/s. Figure 13 shows the results from the survey performed by the sonar attached to the UAV. Sonar covered the same cross-section (depicted in red line) and the mean water depth was

0.90 m. The stream bed is made of concrete at a specific location while sediment deposition is found near the banks.



Figure 9. The study area of Aggitis section near the Simvoli Dam captured by the UAV parallel to the XY plane. There is a bridge (the main road network) and a telemetric hydrologic station (in the yellow circle) to monitor the streamflow for flood events. The red line (cross-section) is 18 m.

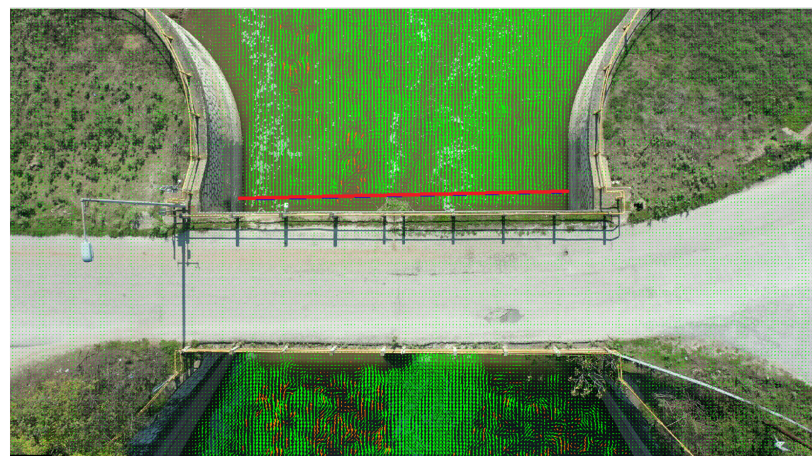


Figure 10. The study area of Aggitis section near the Simvoli Dam captured by the UAV parallel to the XY plane. The green arrows represent the vectors of the surface velocity produced by the PIVlab software (IV-UAV method). The red line (cross-section) is 18 m.

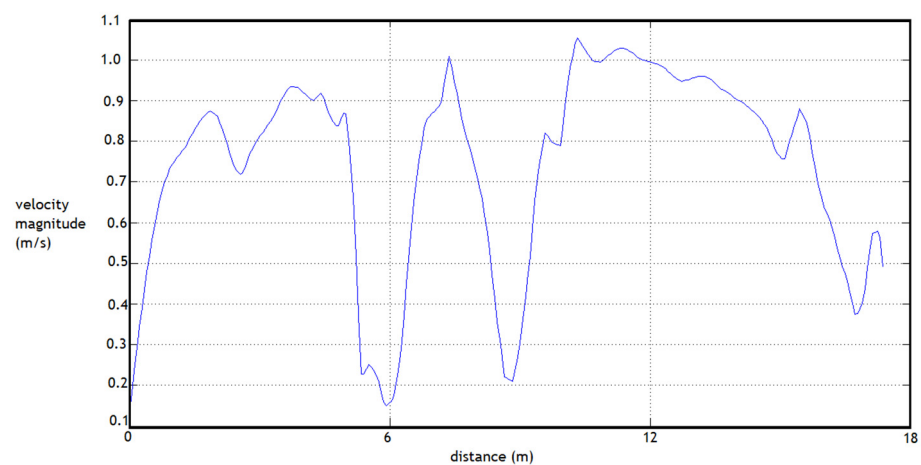


Figure 11. The surface velocity at the cross section as produced by the image analysis in PIVlab.

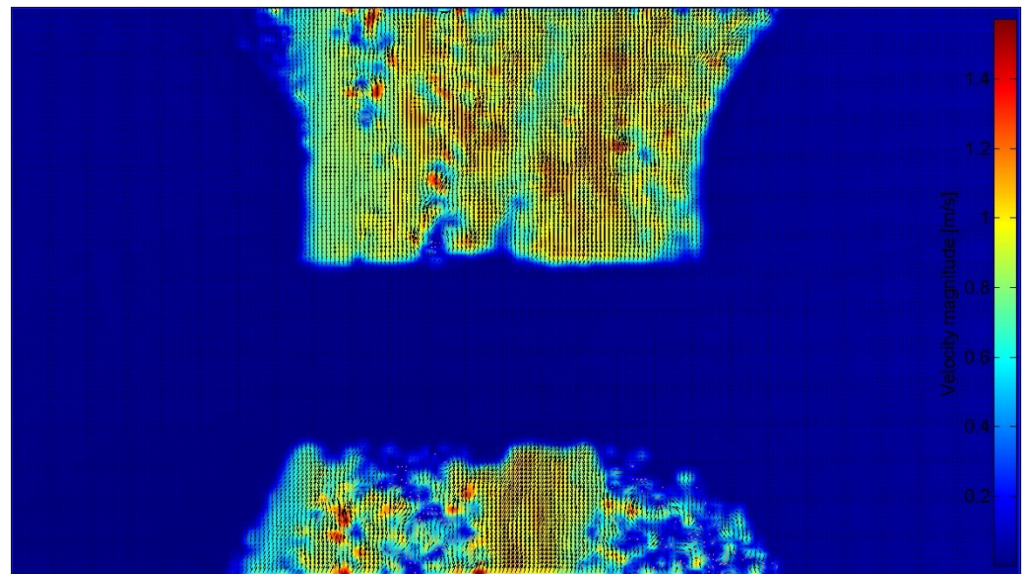


Figure 12. The study reach of Aggitis River near the Simvoli Dam as captured by the UAV parallel to the XY plane. The surface velocity produced by the PIVlab software (IV-UAV method) is depicted in a colorized scale from 0 (blue) to 1.5 (red).

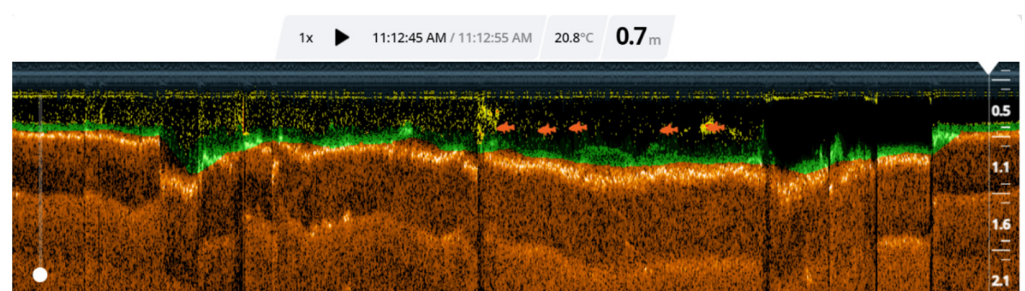


Figure 13. The bathymetric result produced by the sonar survey along the cross section.

In regard to other field measurements, the hydrologic station recorded the mean surface velocity at 0.70 m/s and the water depth at 0.91 m. The subsurface water velocity (with the streamflow meter) was measured at 0.88 m/s while the mean depth based on the tape measure was 0.92 m at the selected cross-section. Thus, the mean discharge (streamflow), based on the current flow meter was measured at 14.57 m³/s, while based on the hydrologic station it was 11.47 m³/s. The streamflow, based on the new method, was estimated at 13.62 m³/s (see Table 3). Finally, Table 4 is a comparative and presents the percentages of differences among the three methodologies utilized in this study.

Table 3. The estimated depth, cross sectional area, velocity and streamflow for the three utilized methodologies.

| Mean Values /Methodology | Streamflow Meter | Hydrologic Station | UAV + Sonar |
|------------------------------------|-------------------------|-------------------------|-------------------------|
| Depth | 0.89 m | 0.91 m | 0.90 m |
| Cross Sectional Area (× 18 meters) | 16.56 m ² | 16.38 m ² | 16.02 m ² |
| Velocity | 0.88 m/s | 0.70 m/s | 0.85 m/s |
| Streamflow | 14.57 m ³ /s | 11.47 m ³ /s | 13.62 m ³ /s |

Table 4. Percentages of difference (%) among the three utilized methodologies.

| | Streamflow Meter | Hydrologic Station | UAV + Sonar |
|-----------------------|-------------------------|-------------------------|-------------------------|
| Streamflow | 14.57 m ³ /s | 11.47 m ³ /s | 13.62 m ³ /s |
| Streamflow Meter | 100% | 78.72% | 93.48 m ² |
| Hydrologic Station | 127.03% | 100% | 118.74% |
| UAV + Sonar | 106.98% | 84.21% | 100% |

4. Discussion and Recommendations

Among the various methods that exist (e.g., traditional velocity–area method, slope–area methods, acoustic Doppler methods) [100] this study showcased an innovative application of IV-UAV in combination with sonar bathymetry in order to acquire quick, easy, and reliable results of streamflow. The specific methodology would have a great impact on streamflow monitoring as well as capturing hydro-geomorphologic changes. The accurate and reliable measurement of stream velocity plays an important role in locating “hot-spots” of soil erosion/deposition along the streambanks and the streambed. Streamflow in natural channels usually varies substantially spatially. Specifically, velocity varies from the surface of the water to the bottom of the streambed, from one side of the bank to the other, along the pool-riffle morphology, and between meanders and straight channels. Generally, water velocity is measured at 60% (100% is the water surface and 0% is the streambed) on vertical velocities [101]. The meandering alters the locations of the strongest and weakest flow resulting in important geomorphic implications for sediment deposition or erosion processes and finally meander migration [102]. In addition, riparian vegetation can significantly influence the morphology of a river, the channel geometry, and the flow dynamics [103–105]. The extensive urbanization observed need to be considered since urban planning/infrastructure engineering highly alter the stream’s kinetics and velocity (e.g., channelization of streambanks, bridge, dams, fish ladders, etc.) [106–108]. Finally, climate change is altering the hydrologic regime and consequently the sediment transport capacity and processes [109]. All the above make it a necessity to find a new tool to be able to measure streamflow faster quicker and most cost-efficient. We believe the method we tested will provide water managing authorities with an easily implemented and user-friendly method.

Streamflow is among the most used methods to estimate the environmental flow of rivers, with the key issue being the choice of appropriate criteria and tools for hydrologic and hydraulic monitoring [110,111]. Environmental flow is the flow regime able to sustain the natural values and services of water and water-dependent ecosystems on the natural watercourses, riparian zones, and their floodplains [112,113]. Environmental flows are essential to developing and implementing sustainable water management and the proposed methodology could make a significant impact by a cost-effective increase of the monitoring locations. Additionally, the European Green Deal could motivate agencies and responsible authorities to adopt this method in order to further implement nature-based solutions (NbS). NbS are defined as “*living solutions inspired by, continuously supported by and using nature, which are designed to address various societal challenges in a resource-efficient and adaptable manner and to provide simultaneously economic, social, and environmental benefits*” [114]. Understanding streamflow dynamics and locations of erosion/deposition processes are critical elements for the proper implementation of nature-based solutions [115]. Specifically, the type of the nature-based solution, its dimensions, and its location (targeted approaches) will help maintain the sustainability of natural streams [116,117].

Future research should include testing the method in different types of streams (e.g., different bed materials, different channel sizes, widths, amount of tree cover and riparian vegetation, slope, etc.). Generally, strong wind and heavy rainfall should be avoided

as it is dangerous to fly the UAV under such conditions. But the advantage is that could go later or the next day. The specific methodology might be more difficult to implement in small order streams if the water depth is too low. In addition, vegetation plays an important role. If the water surface is covered by the tree canopy, it is impossible to record proper images to measure the surface water velocity, while the wire of the sonar is at risk to be tangled with the tree branches. If trying to fly under the tree canopy, the GPS signal might be weak and difficult to hover. Furthermore, the shadows of the tree canopy will induce errors on the water surface for image analysis. In such cases, might have to fly when the leaves have fallen. Larger rivers might be easier as monitoring points since in many cases the width of the channel is quite big and in most cases, there is no closed vegetation canopy, so might be easier to implement. In this case, we must be aware in order to record the total width of the river (including ground control points). To achieve this, the UAV must hover at a higher altitude and this probably would result in weaknesses in image analysis (e.g., the tracers' size may not be enough in order to be visible). We would like to expand also to other types like braided streams. In these cases, we could record how the main water paths of the river change through time and better understand the processes. Generally, we would like to implement the method at ephemeral, intermittent, and perennial streams.

This methodology could be used by water managers to help provide best management practices to reduce erosion and mitigate floods. If the velocity is low and the stream bed is smooth, streams may exhibit laminar flow in which all of the water molecules flow in parallel paths. At higher velocities, the flow is characterized as turbulent flow (water molecules don't follow parallel paths) [118]. Typically, streamflow in natural environments is turbulent. Stream water has the capacity to carry a dissolved load, fine sediments, clay, and silt particles as suspended load, and coarse sands and gravels as bed load. Fine particles will only remain suspended if the flow is turbulent. In laminar flow, suspended particles will slowly settle into the bed [119]. The interaction between a turbulent flow and a granular bed via sediment transport produces various bedforms such as ripples (downstream-propagating transverse bedforms), chevrons and bars (bedforms inclined with respect to the flow direction), and antidunes (upstream-propagating bedforms) [120]. With increasing discharge, the bottom velocity of the pool increases faster than that of the adjacent riffles; thus, the streamflow sorts bedload material in different locations. Specifically, the coarsest material is deposited on the riffles and bars at relatively high flow whereas fines are deposited in pools at relatively low flow [121]. Stream competence refers to the heaviest particles a stream can carry and it highly depends on the stream velocity. Stream capacity is the maximum amount of solid load (bed and suspended) a stream can carry. It depends on both the discharge and the velocity (since velocity affects the competence and therefore the range of particle sizes that may be transported) [122]. During floods when stream velocity and discharge (and therefore competence and capacity) are very high resulting in intense hydro-geomorphologic changes on streambeds and streambanks from bed scouring (erosion), sediment transport (bed and suspended loads), and sediment deposition [123]. Thus, through this methodology by increasing the locations of streamflow measurements along with their frequency greater insight into the hydrologic regimes and fluvio-geomorphic process will be gained. This should lead to the implementation of more water management that are based on more accurate and detailed data that should lead to more sustainability in the long-term and should help mitigate the serious problems that the riverine ecosystem might be facing (e.g., erosion, deposition, flooding).

The innovative method, presented in this paper, improves the ability and reduces the uncertainty in estimating and developing streamflow datasets on natural rivers by using a UAV coupled with a sonar. The method is very easy to be implemented, it needs only the proper certification based on European Union Legislation about UAV pilot license and flight plans regulations/guidelines [124]. An important advantage against other methods is the remote character of the technique. The method can be applied at inaccessible locations and can cover long distances of reach. One of the requirements is to keep clear visibility with the airborne platform for safety rules. In other methods, such as the typically used

streamflow meter along cross-sections, this is time-consuming, while in most cases the monitoring stations are stable. In addition, the installation of a monitoring station at a regular place requires either proper authorization or extra funds for security purposes as they are vulnerable to natural or manmade disasters (even thief issues). The proposed method has the potential to address this challenge through rapid, on-demand, and high-resolution spatial streamflow data [125]. Last but not least, the tools required (both software and hardware) are of low-cost, and in some cases, even free (e.g., the software). This is a major advantage when selecting the best monitoring method in all monitoring cases as well as for hydrologic and hydraulic studies.

This method could be utilized by water managers to achieve sustainable water management (essential to know discharges throughout a year) and also understand better when floods and erosion/deposition occur but also under what conditions (understanding the processes). This should help mitigate the extreme events along the stream banks and bed and the adjacent floodplains. For image velocimetry to be effective, the choice of the velocimetry algorithm and its parameters, and also the design of the measurement setup, camera calibration, general image processing, and signal filtering should be carefully considered and chosen [126]. The absence of densely seeded surfaces (with surface tracers) may lead to consistent flow velocity underestimations in diverse natural conditions [127]. The operator effect is another prominent error source in image-based velocimetry methods (trained personnel need to be hired). Video sampling, ortho-rectification parameters, motion analysis parameters, and filters can also strongly impact velocity and discharge measurements. [128].

Overall, this was a first attempt of implementing a doubling monitoring system on natural rivers, so further study is needed to test the approach in different types of streams as mentioned above. Although the new technique is very promising, the attached sonar system is not a permanent device or cannot be remotely-monitored through a mechanism able to wrap/unroll its wire. For this reason, a telemetric device must be developed that will enable it to act as a cargo delivering platform. This should have attached a motor to stretch or gather the sonar device while simultaneously not affecting the camera field of view for the orthogonal captures (parallel to XY plane). This improvement should significantly improve the utility of the methods and the ease-of-use to the operator.

Author Contributions: Conceptualization, P.K.; methodology, P.K. and G.N.Z.; data curation, P.K.; software, P.K.; validation, P.K.; software analysis, P.K. and G.N.Z.; writing—original draft preparation, P.K.; writing—review and editing, G.N.Z.; visualization, P.K.; project administration, G.N.Z.; funding acquisition, G.N.Z. All authors have read and agreed to the published version of the manuscript.

Funding: This research was funded by the Joint Operational Black Sea Programme 2014–2020 and the Project BSB 963 “Protect-Streams-4-Sea”, with the financial assistance of the European Union. The content of this publication is the sole responsibility of the authors, and in no case should it be considered to reflect the views of the European Union.

Institutional Review Board Statement: Not applicable.

Informed Consent Statement: Not applicable.

Data Availability Statement: Not applicable.

Acknowledgments: To Georgios Gkiatas who helped during field measurements.

Conflicts of Interest: The authors declare no conflict of interest. The funders had no role in the design of the study; in the collection, analyses, or interpretation of data; in the writing of the manuscript; or in the decision to publish the results.

References

1. Zaimes, G.N. Mediterranean riparian areas—climate change implications and recommendations. *J. Environ. Biol.* **2020**, *41*, 957–965. [[CrossRef](#)]
2. Zaimes, G.N.; Iakovoglou, V.; Syropoulos, D.; Kaltsas, D.; Avtzis, D. Assessment of Two Adjacent Mountainous Riparian Areas along Nestos River Tributaries of Greece. *Forests* **2021**, *12*, 1284. [[CrossRef](#)]

3. Pumo, D.; Noto, L.V.; Viola, F. Ecohydrological modelling of flow duration curve in Mediterranean river basins. *Adv. Water Resour.* **2013**, *52*, 314–327. [[CrossRef](#)]
4. Burgi, P.H. Hydraulic design of vertical stilling wells. *J. Hydraul. Div.* **1975**, *101*, 801–816. [[CrossRef](#)]
5. Parshall, R.L. The improved Venturi flume. *Trans. Am. Soc. Civil Eng.* **1926**, *89*, 841–851. [[CrossRef](#)]
6. Mansour, H.A.; Abdallah, E.F.; Gaballah, M.S.; Gyuricza, C. Impact of bubbler discharge and irrigation water quantity on 1-hydraulic performance evaluation and maize biomass yield. *Int. J. GEOMATE* **2015**, *9*, 1538–1544. [[CrossRef](#)]
7. Lamine, B.O.M.; Ferreira, V.G.; Yang, Y.; Ndehedehe, C.E.; He, X. Estimation of the Niger River cross-section and discharge from remotely-sensed products. *J. Hydrol. Reg. Stud.* **2021**, *36*, 100862. [[CrossRef](#)]
8. Pantelakis, D.; Doulgeris, C.; Hatzigiannakis, E.; Arampatzis, G. Evaluation of discharge measurements methods in a natural river of low or middle flow using an electromagnetic flow meter. *River Res. Appl.* **2022**, *38*, 1003–1013. [[CrossRef](#)]
9. Morlot, T.; Perret, C.; Favre, A.C.; Jalbert, J. Dynamic rating curve assessment for hydrometric stations and computation of the associated uncertainties: Quality and station management indicators. *J. Hydrol.* **2014**, *517*, 173–186. [[CrossRef](#)]
10. Westerberg, I.; Guerrero, J.L.; Seibert, J.; Beven, K.J.; Halldin, S. Stage-discharge uncertainty derived with a non-stationary rating curve in the Choluteca River, Honduras. *Hydrol. Processes* **2011**, *25*, 603–613. [[CrossRef](#)]
11. Corato, G.; Ammari, A.; Moramarco, T. Conventional point-velocity records and surface velocity observations for estimating high flow discharge. *Entropy* **2014**, *16*, 5546–5559. [[CrossRef](#)]
12. Tsubaki, R.; Fujita, I.; Tsutsumi, S. Measurement of the flood discharge of a small-sized river using an existing digital video recording system. *J. Hydro-Environ. Res.* **2011**, *5*, 313–321. [[CrossRef](#)]
13. De Girolamo, A.M.; Pappagallo, G.; Porto, A.L. Temporal variability of suspended sediment transport and rating curves in a Mediterranean river basin: The Celone (SE Italy). *Catena* **2015**, *128*, 135–143. [[CrossRef](#)]
14. Kostaschuk, R.; Best, J.; Villard, P.; Peakall, J.; Franklin, M. Measuring flow velocity and sediment transport with an acoustic Doppler current profiler. *Geomorphology* **2005**, *68*, 25–37. [[CrossRef](#)]
15. Boldt, J.A.; Oberg, K.A. Validation of streamflow measurements made with M9 and RiverRay acoustic Doppler current profilers. *J. Hydraul. Eng.* **2016**, *142*, 04015054. [[CrossRef](#)]
16. Wang, X. Advances in separating effects of climate variability and human activity on stream discharge: An overview. *Adv. Water Resour.* **2014**, *71*, 209–218. [[CrossRef](#)]
17. Stone, M.C.; Hotchkiss, R.H. Evaluating velocity measurement techniques in shallow streams. *J. Hydraul. Res.* **2007**, *45*, 752–762. [[CrossRef](#)]
18. Fulton, J.; Ostrowski, J. Measuring real-time streamflow using emerging technologies: Radar, hydroacoustics, and the probability concept. *J. Hydrol.* **2008**, *357*, 1–10. [[CrossRef](#)]
19. Costa, J.E.; Cheng, R.T.; Haeni, F.P.; Melcher, N.; Spicer, K.R.; Hayes, E.; Plant, W.; Hayes, K.; Teague, C.; Barrick, D. Use of radars to monitor stream discharge by noncontact methods. *Water Resour. Res.* **2006**, *42*. [[CrossRef](#)]
20. Gleason, C.J.; Smith, L.C. Toward global mapping of river discharge using satellite images and at-many-stations hydraulic geometry. *Proc. Natl. Acad. Sci. USA* **2014**, *111*, 4788–4791. [[CrossRef](#)]
21. Pavelsky, T.M. Using width-based rating curves from spatially discontinuous satellite imagery to monitor river discharge. *Hydrol. Processes* **2014**, *28*, 3035–3040. [[CrossRef](#)]
22. Kastridis, A.; Stathis, D. Evaluation of hydrological and hydraulic models applied in typical Mediterranean Ungauged watersheds using post-flash-flow measurements. *Hydrology* **2020**, *7*, 12. [[CrossRef](#)]
23. Papaioannou, G.; Efstratiadis, A.; Vasiliades, L.; Loukas, A.; Papalexiou, S.M.; Koukouvinos, A.; Tsoukalas, I.; Kossieris, P. An operational method for flood directive implementation in ungauged urban areas. *Hydrology* **2018**, *5*, 24. [[CrossRef](#)]
24. Tosi, F.; Rocca, M.; Aleotti, F.; Poggi, M.; Mattoccia, S.; Tauro, F.; Toth, E.; Grimaldi, S. Enabling image-based streamflow monitoring at the edge. *Remote Sens.* **2020**, *12*, 2047. [[CrossRef](#)]
25. Pumo, D.; Alongi, F.; Ciraolo, G.; Noto, L.V. Optical methods for river monitoring: A simulation-based approach to explore optimal experimental setup for LSPIV. *Water* **2021**, *13*, 247. [[CrossRef](#)]
26. Tauro, F.; Olivieri, G.; Petroselli, A.; Porfiri, M.; Grimaldi, S. Flow monitoring with a camera: A case study on a flood event in the Tiber River. *Environ. Monit. Assess.* **2016**, *188*, 118. [[CrossRef](#)] [[PubMed](#)]
27. Tauro, F. Particle tracers and image analysis for surface flow observations. *Wiley Interdiscip. Rev. Water* **2016**, *3*, 25–39. [[CrossRef](#)]
28. Admiraal, D.M.; Stansbury, J.S.; Haberman, C.J. Case study: Particle velocimetry in a model of lake Ogallala. *J. Hydraul. Eng.* **2004**, *130*, 599–607. [[CrossRef](#)]
29. Perks, M.T.; Fortunato Dal Sasso, S.; Hauet, A.; Jamieson, E.; Le Coz, J.; Pearce, S.; Peña-Haro, S.; Pizarro, A.; Strelnikova, D.; Tauro, F.; et al. Towards harmonisation of image velocimetry techniques for river surface velocity observations. *Earth Syst. Sci. Data* **2020**, *12*, 1545–1559. [[CrossRef](#)]
30. Fujita, I.; Watanabe, H.; Tsubaki, R. Development of a non-intrusive and efficient flow monitoring technique: The space-time image velocimetry (STIV). *Int. J. River Basin Manag.* **2007**, *5*, 105–114. [[CrossRef](#)]
31. Fujita, I.; Muste, M.; Kruger, A. Large-scale particle image velocimetry for flow analysis in hydraulic engineering applications. *J. Hydraul. Res.* **1998**, *36*, 397–414. [[CrossRef](#)]
32. Patalano, A.; Garcia, C.M.; Brevis, W.; Bleninger, T.; Guillen, N.; Moreno, L.; Rodriguez, A. Recent advances in Eulerian and Lagrangian large-scale particle image velocimetry. In Proceedings of the 36th IAHR World Congress, The Hague, The Netherlands, 28 June–3 July 2015.

33. Jolley, M.J.; Russell, A.J.; Quinn, P.F.; Perks, M.T. Considerations When Applying Large-Scale PIV and PTV for Determining River Flow Velocity. *Front. Water* **2021**, *3*, 709269. [[CrossRef](#)]
34. Manfreda, S.; McCabe, M.F.; Miller, P.E.; Lucas, R.; Pajuelo Madrigal, V.; Mallinis, G.; Ben Dor, E.; Helman, D.; Estes, L.; Ciruolo, G.; et al. On the use of unmanned aerial systems for environmental monitoring. *Remote Sens.* **2018**, *10*, 641. [[CrossRef](#)]
35. Whitehead, K.; Hugenholtz, C.H. Remote sensing of the environment with small unmanned aircraft systems (UASs), part 1: A review of progress and challenges. *J. Unmanned Veh. Syst.* **2014**, *2*, 69–85. [[CrossRef](#)]
36. Schweitzer, S.A.; Cowen, E.A. Instantaneous River-Wide Water Surface Velocity Field Measurements at Centimeter Scales Using Infrared Quantitative Image Velocimetry. *Water Resour. Res.* **2021**, *57*, e2020WR029279. [[CrossRef](#)]
37. Kinzel, P.J.; Legleiter, C.J. sUAS-based remote sensing of river discharge using thermal particle image velocimetry and bathymetric lidar. *Remote Sens.* **2019**, *11*, 2317. [[CrossRef](#)]
38. Le Boursicaud, R.; Pénard, L.; Hauet, A.; Thollet, F.; Le Coz, J. Gauging extreme floods on YouTube: Application of LSPIV to home movies for the post-event determination of stream discharges. *Hydrol Processes* **2016**, *30*, 90–105. [[CrossRef](#)]
39. Hauet, A.; Muste, M.; Ho, H.C. Digital mapping of riverine waterway hydrodynamic and geomorphic features. *Earth Surf. Processes Landf.* **2009**, *34*, 242–252. [[CrossRef](#)]
40. Lewis, Q.W.; Rhoads, B.L. Resolving two-dimensional flow structure in rivers using large-scale particle image velocimetry: An example from a stream confluence. *Water Resour. Res.* **2015**, *51*, 7977–7994. [[CrossRef](#)]
41. Kim, Y.; Muste, M.; Hauet, A.; Krajewski, W.F.; Kruger, A.; Bradley, A. Stream discharge using mobile large-scale particle image velocimetry: A proof of concept. *Water Resour. Res.* **2008**, *44*, W09502. [[CrossRef](#)]
42. Tauro, F.; Petroselli, A.; Arcangeletti, E. Assessment of drone-based surface flow observations. *Hydrol. Processes* **2016**, *30*, 1114–1130. [[CrossRef](#)]
43. Tauro, F.; Porfiri, M.; Grimaldi, S. Orienting the camera and firing lasers to enhance large scale particle image velocimetry for streamflow monitoring. *Water Resour. Res.* **2014**, *50*, 7470–7483. [[CrossRef](#)]
44. Le Coz, J.; Hauet, A.; Pierrefeu, G.; Dramais, G.; Camenen, B. Performance of image-based velocimetry (LSPIV) applied to flash-flood discharge measurements in Mediterranean rivers. *J. Hydrol.* **2010**, *394*, 42–52. [[CrossRef](#)]
45. Jodeau, M.; Bel, C.; Antoine, G.; Bodart, G.; Le Coz, J.; Faure, J.B.; Hauet, A.; Leclercq, F.; Haddad, H.; Legout, C.; et al. New developments of FUDAA-LSPIV, a user-friendly software to perform river velocity measurements in various flow conditions. In Proceedings of the 10th Conference on Fluvial Hydraulics “River Flow 2020”, Delft, The Netherlands, 6–17 July 2020.
46. Dal Sasso, S.F.; Pizarro, A.; Manfreda, S. Recent Advancements and Perspectives in UAS-Based Image Velocimetry. *Drones* **2021**, *5*, 81. [[CrossRef](#)]
47. Manfreda, S.; Dal Sasso, S.F.; Pizarro, A.; Tauro, F. New insights offered by UAS for river monitoring. In *Applications of Small Unmanned Aircraft Systems: Best Practices and Case Studies*; Sharma, J.B., Ed.; CRC Press, Taylor and Francis Group: New York, NY, USA, 2019; pp. 211–234.
48. Strelnikova, D.; Paulus, G.; Käfer, S.; Anders, K.H.; Mayr, P.; Mader, H.; Scherling, U.; Schneeberger, R. Drone-based optical measurements of heterogeneous surface velocity fields around fish passages at hydropower dams. *Remote Sens.* **2020**, *12*, 384. [[CrossRef](#)]
49. Koutalakis, P. Development of Image-Based Velocimetry and Methodology to Map Geomorphologic Changes on Riverbeds by Utilizing Images/Video Captured by Unmanned Aerial Vehicles. Ph.D. Thesis, University of the Aegean, Mytilene, Greece, 2021.
50. Fujita, I.; Aya, S. Refinement of LSPIV technique for monitoring river surface flows. In Proceedings of the Joint Conference on Water Resource Engineering and Water Resources Planning and Management 2000: Building Partnerships, Minneapolis, MN, USA, 30 July–2 August 2000; pp. 1–9.
51. Kantoush, S.A.; Schleiss, A.J.; Sumi, T.; Murasaki, M. LSPIV implementation for environmental flow in various laboratory and field cases. *J. Hydro-Environ. Res.* **2011**, *5*, 263–276. [[CrossRef](#)]
52. Pearce, S.; Ljubičić, R.; Peña-Haro, S.; Perks, M.; Tauro, F.; Pizarro, A.; Dal Sasso, S.F.; Strelnikova, D.; Grimaldi, S.; Maddock, I.; et al. An evaluation of image velocimetry techniques under low flow conditions and high seeding densities using unmanned aerial systems. *Remote Sens.* **2020**, *12*, 232. [[CrossRef](#)]
53. Meselhe, E.A.; Peeva, T.; Muste, M.V.I. Large scale particle image velocimetry for low velocity and shallow water flows. *J. Hydrol. Eng.* **2004**, *130*, 937–940. [[CrossRef](#)]
54. Detert, M.; Weitbrecht, V. A low-cost airborne velocimetry system: Proof of concept. *J. Hydraul. Res.* **2015**, *53*, 532–539. [[CrossRef](#)]
55. Tauro, F.; Piscopia, R.; Grimaldi, S. Streamflow observations from cameras: Large-scale particle image velocimetry or particle tracking velocimetry? *Water Resour. Res.* **2017**, *53*, 10374–10394. [[CrossRef](#)]
56. Tauro, F.; Porfiri, M.; Grimaldi, S. Surface flow measurements from drones. *J. Hydrol.* **2016**, *540*, 240–245. [[CrossRef](#)]
57. Lewis, Q.W.; Rhoads, B.L. LSPIV measurements of two-dimensional flow structure in streams using small unmanned aerial systems: 1. Accuracy assessment based on comparison with stationary camera platforms and in-stream velocity measurements. *Water Resour. Res.* **2018**, *54*, 8000–8018. [[CrossRef](#)]
58. Lewis, Q.W. Measuring Flow and Mixing at Stream Confluences Using Large-Scale Particle Image Velocimetry, In-Stream Techniques, and Small Unmanned Aerial Systems. Ph.D. Thesis, University of Illinois at Urbana-Champaign, Urbana-Champaign, IL, USA, 2018.
59. Huang, W.C.; Young, C.C.; Liu, W.C. Application of an automated discharge imaging system and LSPIV during typhoon events in Taiwan. *Water* **2018**, *10*, 280. [[CrossRef](#)]

60. Creëlle, S.; Roldan, R.; Herremans, A.; Meire, D.; Buis, K.; Meire, P.; Van Oyen, T.; De Mulder, T.; Troch, P. Validation of large-scale particle image velocimetry to acquire free-surface flow fields in vegetated rivers. *J. Appl. Water Eng. Res.* **2018**, *6*, 171–182. [CrossRef]
61. Fairley, I.; Williamson, B.J.; McIlvenny, J.; King, N.; Masters, I.; Lewis, M.; Neill, S.; Glasby, D.; Coles, D.; Powel, B.; et al. Drone-based large-scale particle image velocimetry applied to tidal stream energy resource assessment. *Renew. Energy* **2022**, *196*, 839–855. [CrossRef]
62. Lewis, Q.W.; Lindroth, E.M.; Rhoads, B.L. Integrating unmanned aerial systems and LSPIV for rapid, cost-effective stream gauging. *J. Hydrol.* **2018**, *560*, 230–246. [CrossRef]
63. Kantoush, S.A.; Schleiss, A.J. Large-scale PIV surface flow measurements in shallow basins with different geometries. *J. Vis.* **2009**, *12*, 361–373. [CrossRef]
64. Shi, Y. Smart cameras for machine vision. In *Smart Cameras*; Belbachir, A.N., Ed.; Springer: Boston, MA, USA, 2009; pp. 283–303.
65. Dal Sasso, S.F.; Pizarro, A.; Pearce, S.; Maddock, I.; Manfreda, S. Increasing LSPIV performances by exploiting the seeding distribution index at different spatial scales. *J. Hydrol.* **2021**, *598*, 126438. [CrossRef]
66. Mandlbürger, G. Bathymetry from images, LiDAR, and Sonar. *PFG–J. Photogramm. Remote Sens. Geoinf. Sci.* **2021**, *89*, 69–70. [CrossRef]
67. Bandini, F.; Kooij, L.; Mortensen, B.K.; Caspersen, M.B.; Olesen, D.; Bauer-Gottwein, P. Mapping inland water bathymetry with Ground Penetrating Radar (GPR) on board Unmanned Aerial Systems (UASs). *Res. Sq.* **2021**. Preprints.. [CrossRef]
68. Lin, Y.C.; Ho, H.C.; Lee, T.A.; Chen, H.Y. Application of Image Tech-nique to Obtain Surface Velocity and Bed Elevation in Open-Channel Flow. *Water* **2022**, *14*, 1895. [CrossRef]
69. Rossi, L.; Mammi, I.; Pelliccia, F. UAV-derived multispectral bathymetry. *Remote Sens.* **2020**, *12*, 3897. [CrossRef]
70. Matsuba, Y.; Sato, S. Nearshore bathymetry estimation using UAV. *Coast. Eng.* **2018**, *60*, 51–59. [CrossRef]
71. Sanjou, M.; Kato, K.; Aizawa, W.; Okamoto, T. Development of drone-type float for surface-velocity measurement in rivers. *Environ. Fluid Mech.* **2022**, *22*, 955–969. [CrossRef]
72. Lubczonek, J.; Kazimierski, W.; Zaniewicz, G.; Lacka, M. Methodology for combining data acquired by unmanned surface and aerial vehicles to create digital bathymetric models in shallow and ultra-shallow waters. *Remote Sens.* **2021**, *14*, 105. [CrossRef]
73. Erena, M.; Atenza, J.F.; García-Galiano, S.; Domínguez, J.A.; Bernabé, J.M. Use of drones for the topo-bathymetric monitoring of the reservoirs of the Segura River Basin. *Water* **2019**, *11*, 445. [CrossRef]
74. Zinke, P.; Flener, C. Experiences from the use of unmanned aerial vehicles (UAV) for river bathymetry modelling in Norway. *Vann* **2013**, *48*, 351–360.
75. Bandini, F.; Olesen, D.; Jakobsen, J.; Kittel, C.M.M.; Wang, S.; Garcia, M.; Bauer-Gottwein, P. Bathymetry observations of inland water bodies using a tethered sing-beam sonar controlled by an Unmanned Aerial Vehicle. *Hydrol. Earth Syst. Sci.* **2008**, *25*, 4549–4565.
76. Ruffell, A.; Lally, A.; Rocke, B. Dronar—Geoforensic Search Sonar from a Drone. *Forensic Sci.* **2021**, *1*, 202–212. [CrossRef]
77. Bandini, F.; Bauer-Gottwein, P.; Garcia, M. Hydraulics and Drones: Observations of Water Level, Bathymetry and Water Surface Velocity from Unmanned Aerial Vehicles. Ph.D. Thesis, Technical University of Denmark, Lyngby, Denmark, 2017.
78. Astaras, T. The Gorge of the Angitis River at “Stena Petras” Near the Alistrati Cave. A Magnificent Piece of Natural Architecture in Eastern Macedonia, Greece. In *Natural Heritage from East to West: Case Studies from 6 Countries*; Evelpidou, N., de Figueiredo, T., Mauro, F., Tecim, V., Vassilopoulos, A., Eds.; Springer: Berlin/Heidelberg, Germany, 2010; pp. 51–57.
79. Koutalakis, P.; Tzoraki, O.; Zaimes, G.N. Detecting riverbank changes with remote sensing tools. Case study: Aggitis River in Greece. *Ann. Dunarea Jos Univ. Galati Fascicle II Math. Phys. Theor. Mech.* **2019**, *42*, 134–142. [CrossRef]
80. Pennos, C.; Lauritzen, S.E.; Pechlivanidou, S.; Sotiriadis, Y. Geomorphic constrains on the evolution of the Aggitis River Basin Northern Greece (a preliminary report). *BGSJ* **2016**, *50*, 365–373. [CrossRef]
81. Georgakopoulos, A.; Fernández-Turiel, J.; Christanis, K.; Kalaitzidis, S.; Kasso-li-Fournaraki, A.; Llorens, J.; Filippidis, A.; Gimeno, D. The Drama basin water: Quality and peat/lignite interaction. *Environ. Geol.* **2001**, *41*, 121–127. [CrossRef]
82. Schismenos, S.; Stevens, G.J.; Georgeou, N.; Emmanouloudis, D.; Shrestha, S.; Thapa, B.S.; Gurung, S. Flood and Renewable Energy Humanitarian Engineering Research: Lessons from Aggitis, Greece and Dhuskun, Nepal. *Geosci. J.* **2022**, *12*, 71. [CrossRef]
83. Bartzoudis, G. *The Hydraulic Works in the Plain of Serres, Greece*; Reprint March 2021; Serres, Greece, 1994. (In Greek)
84. Liu, W.C.; Lu, C.H.; Huang, W.C. Large-scale particle image velocimetry to measure streamflow from videos recorded from unmanned aerial vehicle and fixed imaging system. *Remote Sens.* **2021**, *13*, 2661. [CrossRef]
85. DJI Phantom Pro Specifications. Available online: <https://www.dji.com> (accessed on 24 May 2022).
86. Bogoyavlensky, V.; Bogoyavlensky, I.; Nikonov, R.; Kishankov, A. Complex of geophysical studies of the Seyakha catastrophic gas blowout crater on the Yamal Peninsula, Russian Arctic. *Geosci. J.* **2020**, *10*, 215. [CrossRef]
87. Maiakovska, O.; Andriantsoa, R.; Tönges, S.; Legrand, C.; Gutekunst, J.; Hanna, K.; Pârvulescu, L.; Novitsky, R.; Weiperth, A.; Sciberras, A.; et al. Genome analysis of the monoclinal marbled crayfish reveals genetic separation over a short evolutionary timescale. *Commun. Biol.* **2021**, *4*, 74. [CrossRef]
88. Giambastiani, Y.; Giusti, R.; Cecchi, S.; Palomba, F.; Manetti, F.; Romanelli, S.; Bottai, L. Volume estimation of lakes and reservoirs based on aquatic drone surveys: The case study of Tuscany, Italy. *J. Water Land Dev.* **2020**, *46*, 84–96.
89. Szlapińska, S.; Tokarczyk, R. A Comparison of Accuracy between Point Clouds from Convergent Images and Spherical Panoramas. *Geomat. Environ. Eng.* **2017**, *11*, 63–72. [CrossRef]

90. Fang, W.; Zheng, L. Distortion correction modeling method for zoom lens cameras with bundle adjustment. *J. Opt. Soc. Korea* **2016**, *20*, 140–149. [[CrossRef](#)]
91. Hedborg, J.; Ringaby, E.; Forssén, P.E.; Felsberg, M. Structure and motion estimation from rolling shutter video. In Proceedings of the IEEE International Conference on Computer Vision Workshops (ICCV Workshops), Barcelona, Spain, 6–13 November 2011; pp. 17–23.
92. Tsai, T.H.; Fang, C.L.; Chuang, H.M. Design and implementation of efficient video stabilization engine using maximum a posteriori estimation and motion energy smoothing approach. *IEEE Trans. Circuits Syst. Video Technol.* **2011**, *22*, 817–830. [[CrossRef](#)]
93. Walha, A.; Wali, A.; Alimi, A.M. Video stabilization with moving object detecting and tracking for aerial video surveillance. *Multimed. Tools Appl.* **2015**, *74*, 6745–6767. [[CrossRef](#)]
94. Koutalakis, P.; Tzoraki, O.; Zaimes, G.N. Software utilized for image-based velocimetry methods focused on water resources. *Desalin. Water Treat.* **2021**, *218*, 1–17. [[CrossRef](#)]
95. Thielicke, W.; Stamhuis, E. PIVlab—Towards user-friendly, affordable and accurate digital particle image velocimetry in MATLAB. *J. Open Res. Softw.* **2014**, *2*, p.e30. [[CrossRef](#)]
96. Koutalakis, P.; Tzoraki, O.; Zaimes, G. UAVs for hydrologic scopes: Application of a low-cost UAV to estimate surface water velocity by using three different image-based methods. *Drones* **2019**, *3*, 14. [[CrossRef](#)]
97. Cao, L.; Weitbrecht, V.; Li, D.; Detert, M. Airborne Feature Matching Velocimetry for surface flow measurements in rivers. *J. Hydraul. Res.* **2021**, *59*, 637–650. [[CrossRef](#)]
98. Patalano, A.; García, C.M. RIVeR—Towards affordable, practical and user-friendly toolbox for Large Scale PIV and PTV techniques. In Proceedings of the International Conference on Fluvial Hydraulics “River Flow 2016”, St. Louis, MO, USA, 11–14 July 2016; pp. 576–579.
99. Ioli, F.; Pinto, L.; Passoni, D.; Nova, V.; Detert, M. Evaluation of Airborne Image Velocimetry approaches using low-cost UAVs in riverine environments. *Int. Arch. Photogramm. Remote Sens. Spat. Inf. Sci.—ISPRS Arch.* **2020**, *43*, 597–604. [[CrossRef](#)]
100. Gore, J.A.; Banning, J. Chapter 3—Discharge measurements and streamflow analysis. In *Methods in Stream Ecology*, 3rd ed.; Hauer, F.R., Lamberti, G.A., Eds.; Academic Press: Cambridge, MA, USA, 1996; pp. 49–70.
101. Gravelle, R. Discharge estimation: Techniques and equipment. In *Geomorphological Techniques*; (Online Edition), Chapter: 3.3.5; Clarke, L.E., Nield, J.M., Eds.; British Society for Geomorphology: London, UK, 2015; Volume 5, pp. 1–8.
102. Ferguson, R.I.; Parsons, D.R.; Lane, S.N.; Hardy, R.J. Flow in meander bends with recirculation at the inner bank. *Water Resour. Res.* **2003**, *39*. [[CrossRef](#)]
103. Nilsson, C. Distribution of stream-edge vegetation along a gradient of current velocity. *J. Ecol.* **1987**, *75*, 513–522. [[CrossRef](#)]
104. Huang, H.Q.; Nanson, G.C. Vegetation and channel variation; a case study of four small streams in southeastern Australia. *Geomorphology* **1997**, *18*, 237–249. [[CrossRef](#)]
105. Gran, K.; Paola, C. Riparian vegetation controls on braided stream dynamics. *Water Resour. Res.* **2001**, *37*, 3275–3283. [[CrossRef](#)]
106. Beschta, R.L.; Platts, W.S. Morphological Features of Small Streams: Significance and Function. *J. Am. Water Resour. Assoc.* **1986**, *22*, 369–379. [[CrossRef](#)]
107. Bell, J.M.; Simonson, A.M.; Fisher, I.J. *Urban Hydrology—Science Capabilities of the U.S. Geological Survey*; Northeast Region Urban Landscape Capabilities Team; Fact Sheet 2016-3023; U.S. Geological Survey: Reston, VA, USA, 2016. [[CrossRef](#)]
108. Hohensinner, S.; Hauer, C.; Muhar, S. River morphology, channelization, and habitat restoration. Riverine ecosystem management. In *Riverine Ecosystem Management*; Schmutz, S., Sendzimirpringer, J., Eds.; Springer: Cham, Switzerland, 2018; pp. 41–65.
109. Zaimes, G.N.; Gounaridis, D.; Symeonakis, E. Assessing the impact of dams on riparian and deltaic vegetation using remotely-sensed vegetation indices and Random Forests modelling. *Ecol. Indic.* **2019**, *103*, 630–641. [[CrossRef](#)]
110. Książek, L.; Woś, A.; Florek, J.; Wyrębek, M.; Młyński, D.; Wałęga, A. Combined use of the hydraulic and hydrological methods to calculate the environmental flow: Wisłoka river, Poland: Case study. *Environ. Monit. Assess.* **2019**, *191*, 254. [[CrossRef](#)] [[PubMed](#)]
111. Whiting, P.J. Streamflow necessary for environmental maintenance. *Annu. Rev. Earth Planet. Sci.* **2002**, *30*, 181. [[CrossRef](#)]
112. Tharme, R.E. A global perspective on environmental flow assessment: Emerging trends in the development and application of environmental flow methodologies for rivers. *River Res. Appl.* **2003**, *19*, 397–441. [[CrossRef](#)]
113. Merritt, D.M.; Scott, M.L.; LeRoy Poff, N.; Auble, G.T.; Lytle, D.A. Theory, methods and tools for determining environmental flows for riparian vegetation: Riparian vegetation-flow response guilds. *Freshw. Biol.* **2010**, *55*, 206–225. [[CrossRef](#)]
114. Maes, J.; Jacobs, S. Nature-based solutions for Europe’s sustainable development. *Conserv. Lett.* **2017**, *10*, 121–124. [[CrossRef](#)]
115. Gonzalez-Ollauri, A. Sustainable Use of Nature-Based Solutions for Slope Protection and Erosion Control. *Sustainability* **2022**, *14*, 1981. [[CrossRef](#)]
116. Guerrero, P.; Haase, D.; Albert, C. Locating spatial opportunities for nature-based solutions: A river landscape application. *Water* **2018**, *10*, 1869. [[CrossRef](#)]
117. Iakovoglou, V.; Koutalakis, P.; Diaconu, D.; Tufekcioglu, M.; Trombitsky, I.; Ghulijanyan, A.; Zaimes, G.N. Nature-based solutions for streams to reduce sediment and litter pollution in the Black Sea. In Proceedings of the Environmental Challenges in the Black Sea Basin: Impact on Human Health, Galati, Romania, 23–26 September 2020.
118. Vogel, S. *Life in Moving Fluids: The Physical Biology of Flow-Revised and Expanded*, 2nd ed.; Princeton University Press: Princeton, NJ, USA, 2020; pp. 47–50.
119. Strahler, A.N. Dynamic basis of geomorphology. *Geol. Soc. Am. Bull.* **1952**, *63*, 923–938. [[CrossRef](#)]

120. Andreotti, B.; Claudin, P.; Devauchelle, O.; Durán, O.; Fourrière, A. Bedforms in a turbulent stream: Ripples, chevrons and antidunes. *J. Fluid Mech.* **2012**, *690*, 94–128. [[CrossRef](#)]
121. Keller, E.A. Areal sorting of bed-load material: The hypothesis of velocity reversal. *Geol. Soc. Am. Bull.* **1971**, *82*, 753–756. [[CrossRef](#)]
122. Kaffas, K.; Hrissanthou, V. Computation of hydro-geomorphologic changes in two basins of northeastern Greece. In *Hydro-Geomorphology-Models and Trends*; Shukla, D.P., Ed.; IntechOpen: London, UK, 2017; pp. 9–32.
123. Rusnák, M.; Goga, T.; Michaleje, L.; Šulc Michalková, M.; Máchka, Z.; Bertalan, L.; Kidová, A. Remote Sensing of Riparian Ecosystems. *Remote Sens.* **2022**, *14*, 2645. [[CrossRef](#)]
124. Bassi, E. European drones regulation: Today's legal challenges. In Proceedings of the International Conference on Unmanned Aircraft Systems (ICUAS), Atlanta, GA, USA, 11–14 June 2019.
125. McDonald, W. Drones in urban stormwater management: A review and future perspectives. *Urban Water J.* **2019**, *16*, 505–518. [[CrossRef](#)]
126. Detert, M. How to avoid and correct biased riverine surface image velocimetry. *Water Resour. Res.* **2021**, *57*, e2020WR027833. [[CrossRef](#)]
127. Tauro, F.; Petroselli, A.; Grimaldi, S. Optical sensing for stream flow observations: A review. *J. Agric. Eng.* **2018**, *49*, 199–206. [[CrossRef](#)]
128. Bodart, G.; Le Coz, J.; Jodeau, M.; Hauet, A. Quantifying the operator effect in LSPIV image-based velocity and discharge measurements. In Proceedings of the EGU General Assembly 2022, Vienna, Austria, 23–27 May 2022.